U.S. Army Research Laboratory

SUMMER RESEARCH TECHNICAL REPORT

Microstructural Investigation and Evaluation of Mechanical Properties in Friction Stir Welded Joints

BRIAN JUSTUSSON
MENTORS: DR. CONSTANTINE FOUNTZOULAS AND DR. CHIAN-FONG YEN
U.S. ARMY RESEARCH LABORATORY, WMRD, RDRL-WMM-B,
ABERDEEN PROVING GROUND, MD 21005-5069

Report Documentation Page

Form Approved
OMB No. 0704-0188

1. REPORT DATE	2. REPORT TYPE	3. DATES COVERED
AUG 2011		**00-00-2011 to 00-00-2011**

4. TITLE AND SUBTITLE	5a. CONTRACT NUMBER
Microstructural Investigation And Evaluation Of Mechanical Properties In Friction Stir Welded Joints	5b. GRANT NUMBER
	5c. PROGRAM ELEMENT NUMBER
6. AUTHOR(S)	5d. PROJECT NUMBER
	5e. TASK NUMBER
	5f. WORK UNIT NUMBER
7. PERFORMING ORGANIZATION NAME(S) AND ADDRESS(ES) **U. S. Army Research Labortory,WMRD, RDRL-WMM-B,Aberdeen Proving Ground,MD,21005**	8. PERFORMING ORGANIZATION REPORT NUMBER
9. SPONSORING/MONITORING AGENCY NAME(S) AND ADDRESS(ES)	10. SPONSOR/MONITOR'S ACRONYM(S)
	11. SPONSOR/MONITOR'S REPORT NUMBER(S)

12. DISTRIBUTION/AVAILABILITY STATEMENT
Approved for public release; distribution unlimited

13. SUPPLEMENTARY NOTES
See also ADA548876

14. ABSTRACT

With involvement of the United States Military in various places in the world, increased improvements in personnel and vehicle protection are needed. Traditionally, armoring techniques have performed well against particular threats; however, a new threat has emerged from improvised explosive devices (IEDs), which has exposed the vulnerability of the undercarriage of the vehicle to explosions. Various solutions have been proposed to combat this problem, such as implementation of a unibody construction of the chassis. While traditional joining techniques have shown promise, the variability in mechanical properties of the weldment can be costly and needs to be addressed. Friction Stir Welding (FSW) is a solid-state welding technique, which involves local softening of the material subjected to severe plastic deformation, coupled with a localized heat flux, creates a unique microstructure in and around the weld that is dependent on the FSW parameters. The current work involves the characterization of the microstructures that develop during FSW as it relates to the locally spatial mechanical properties in the weld zone. The microstructure will be characterized by using scanning electron microscopy (SEM) and electron backscatter diffraction (EBSD) techniques, which, when coupled with mechanical testing data, can be used to shed light on the spatial stress-strain behavior of the welded sample.

15. SUBJECT TERMS

16. SECURITY CLASSIFICATION OF:			17. LIMITATION OF ABSTRACT	18. NUMBER OF PAGES	19a. NAME OF RESPONSIBLE PERSON
a. REPORT **unclassified**	b. ABSTRACT **unclassified**	c. THIS PAGE **unclassified**	**Same as Report (SAR)**	**20**	

Contents

List of Figures

List of Tables

Abstract

With involvement of the United States Military in various places in the world, increased improvements in personnel and vehicle protection are needed. Traditionally, armoring techniques have performed well against particular threats; however, a new threat has emerged from improvised explosive devices (IEDs), which has exposed the vulnerability of the undercarriage of the vehicle to explosions. Various solutions have been proposed to combat this problem, such as implementation of a unibody construction of the chassis. While traditional joining techniques have shown promise, the variability in mechanical properties of the weldment can be costly and needs to be addressed. Friction Stir Welding (FSW) is a solid-state welding technique, which involves local softening of the material subjected to severe plastic deformation, coupled with a localized heat flux, creates a unique microstructure in and around the weld that is dependent on the FSW parameters. The current work involves the characterization of the microstructures that develop during FSW as it relates to the locally spatial mechanical properties in the weld zone. The microstructure will be characterized by using scanning electron microscopy (SEM) and electron backscatter diffraction (EBSD) techniques, which, when coupled with mechanical testing data, can be used to shed light on the spatial stress-strain behavior of the welded sample.

Acknowledgments

I am grateful for the support of all the employees of the U.S. Army Research Laboratory (ARL), but in particular of Dr. Constantine Fountzoulas and Dr. Chian-Fong Yen for their continued mentorship and encouragement to become a better research scientist. I am also grateful for the training and general help provided by Dr. Jian Yu, Dr. Brian Shuster, and Dr. Tomoko Sano. Additional help was provided by David Gray, Theresa Dillon, Ashiq Quabili, and Seth Ghiorse. A special thanks goes to Jessica Medintz, who was a valued partner on this work, and Dr. Mark Pankow of ARL and The University of Michigan for helping train my mind to be the research scientist I am today.

Student Bio

I am a third-year Ph.D. pre-candidate at the University of Michigan in Mechanical Engineering, mentored by Prof. Anthony Waas. I currently hold a master's degree in Mechanical Engineering from The University of Southern California and a bachelor's degree from The University of Michigan in Mechanical Engineering. My current research involves the rate-dependent mechanical properties of composites materials, but also in some metals. After completion of my Ph.D. work, my objectives are to continue expanding my current research interests as part of a recognized institution and work in a research laboratory in either the public or private sector, but also, at some point in the future, become a collegiate lecturer.

1. Introduction/Background

Aluminum is becoming an increasingly desirable structural metal for replacing steel due to its lower density, 2.67g/cc and 7.87 g/cc, respectively, with comparable specific bending stiffness. To date, armored vehicles rely heavily on steel armor, which increases the vehicle payload. To replace steel with light metals, there is a need for new lightweight personal and vehicular armoring techniques. The creation of a unibody aluminum chassis for armored vehicles can greatly reduce the weight of the vehicle; however, a joining process is needed.

Friction stir welding (FSW) is a solid-state joining technique developed in 1991 (*1*) and currently used extensively in aluminum alloys. This process involves the use of a welding tool, which consists of concentric cylinders composed of a thinner cylinder, known as a pin, and a wider cylinder known as a shoulder (figure 1). The pin is pushed into the material after a critical temperature is reached and the flow stress is easily overcome due to local softening as a result of the heat flux and the tool can be pulled through the material. As the tool is pulled through the material, distinct and unique microstructures develop.

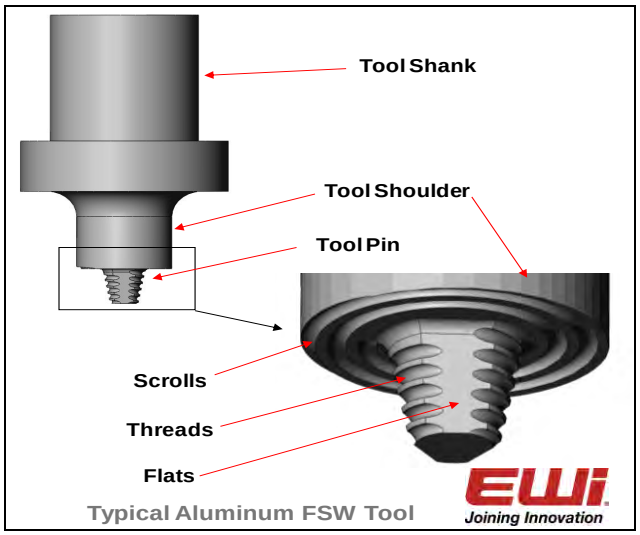

Figure 1. FSW tool.

These microstructures are generally referred to as the Heat Affected Zone (HAZ), which is a result of the heat dissipating through the material, which promotes grain growth, or the Thermo-Mechanically Affected Zone (TMAZ), which is a result of competing mechanisms due to the local heat flux promoting grain growth and localized severe plastic deformation, which results in decreased grain size. A final unique microstructure, termed the weld-nugget, is a fine, equiaxed grain structure located near the center of the weld. These zones have been shown to display unique mechanical properties (*2*), where the yield strength and ultimate tensile strength can be reduced while the ductility remains largely constant. Studies have shown that the microstructures

are a result of dynamic recrystallization and are very dependent on the stir parameters. Hirata et al. (*3*) showed that grain size decreases with weld velocity and increases with rotational speed. As of today, weldability and survivability of welds of advanced aluminum alloys subjected to blast loading have not been established. There is a need to accurately simulate FSW processes to create predictive models for blast loading.

Finite element models have been created to capture the FSW process. Sequential work by Fratini and Buffa (*4–6*) has been able to accurately simulate the various zones in welds of a quarter inch, while capturing the effects of recrystallization. Additional work by Grujicic et al. (*7–8*) was able to simulate FSW of AA-5083 and AA-2139 and clearly identify the development of microstructures. The developed model has been validated through experimental hardness tests (*9*). These models predict the results well, but are very computationally expensive.

The goal of this work is to understand the property distribution in and around the weldment for implementation into the finite models to reduce computational costs and develop a representative response of the weld zone. This will allow for development of a cohesive element to be used in all future simulations. The current work reports the following:

1. The spatial stress-strain response and mechanical properties models
2. The spatial distribution of the grains, grain size, and grain structure
3. Identification of microstructures that lead to variations in spatial mechanical properties

2. Experiment/Calculations

2.1 Material

Two plates of Aluminum 2139 were welded together as a butt joint using the parameters shown in table 1, which have been shown to be optimal parameters in past welds. The single plate was welded at EWI in Dayton, OH. The FSW tool was a two-piece tool with four flats and a left-handed thread, similar to the one shown in figure 1. Global tensile and bending tests were performed at EWI for the weld and were determined to be within specification for weld quality.

Table 1. FSW parameters.

Parameter	Specification
Shoulder diameter	1.625 in
Pin length	0.972 in
Plunge depth	0.65–0.005 in
Spindle speed	150–250 RPM
Travel speed	2 IPM
Total length	18 in

2.2 Grinding/Polishing Method

Polishing was completed using a Stuer RotoPol-31 fitted with Stuer Rotoforce 4 automatic polisher head using the steps shown in table 2. The grinding steps involved sandpaper with the given grit size. The polishing steps for 6 and 3 microns were performed on trident polishing cloths with water-based diamond suspension solutions. The final step for 0.05 micron was performed using colloidal silica. Between steps, the specimens were examined for scratches and cleaned using ethanol. A sodium hydroxide (NaOH) etchant was used for an application time of 1.5 min.

Table 2. Polishing procedure.

Step Type (Grit)	Time (min)
Grinding (120 paper)	Until flat
Grinding (320 paper)	1:30
Grinding (600 paper)	6:00
Grinding (1200 paper)	8:30
Polishing (6 um)	10:00
Polishing (3 um)	15:00
Polishing (0.05 um)	2:00

2.3 Tensile Testing Method

Tensile testing was performed on a screw-driven Instron 1125. Dog bone samples from the plate discussed in section 2.1 were cut using electric discharge machining (EDM) at various places in the weldment. Specimens were cut along the weld (Y), perpendicular to the weld (X), and through thickness (Z). The test was displacement controlled at a rate of 0.004 in/min (0.1 mm/min) to create a quasi-static loading condition. Photos were taken every 15 s using a Nikon D300. The resulting force/displacement data were analyzed and correlated to the photographs using ARAMIS digital image correlation software.

2.4 Microscopy/EBSD Method

Polished samples were examined for grain structures as a function of distance from the weld. Samples were imaged using a Nikon EPIShot 300. Electron backscatter diffraction (EBSD) was performed using a Nova NanoSEM 600. Images were taken with a step size of 1 micrometer and an image space of 250x250 micrometers was used. Images were analyzed using software ,which allows for pole analysis to show how the grains are oriented and textured.

3. Results and Discussion

3.1 Tensile Results

The results of the mechanical testing showed an interesting behavior, as seen in figures 2, 3, and 4. Figure 2 shows the tensile results in X or transverse direction, whereas figure 3 shows the Y or longitudinal direction and figure 4 shows the through thickness results. Of particular interest, groups 2 and 3 show the highest failure strain, but the lowest ultimate tensile strength. This is directly a result of where the samples were taken from. Sample 2 is taken inside of the weldment, whereas sample 3 was taken from an area along the weldment but contained both areas of the weldment and outside.

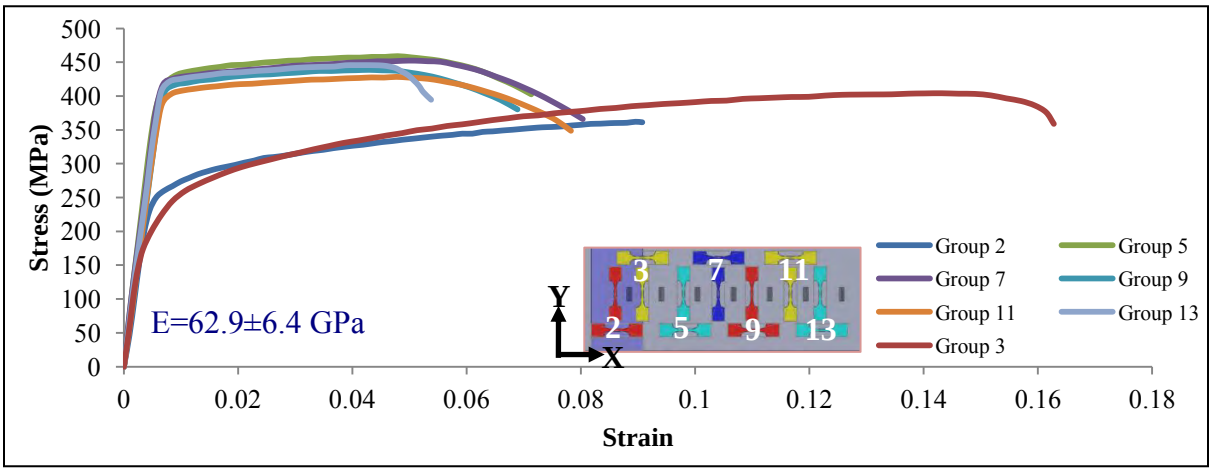

Figure 2. Tensile results in X-direction.

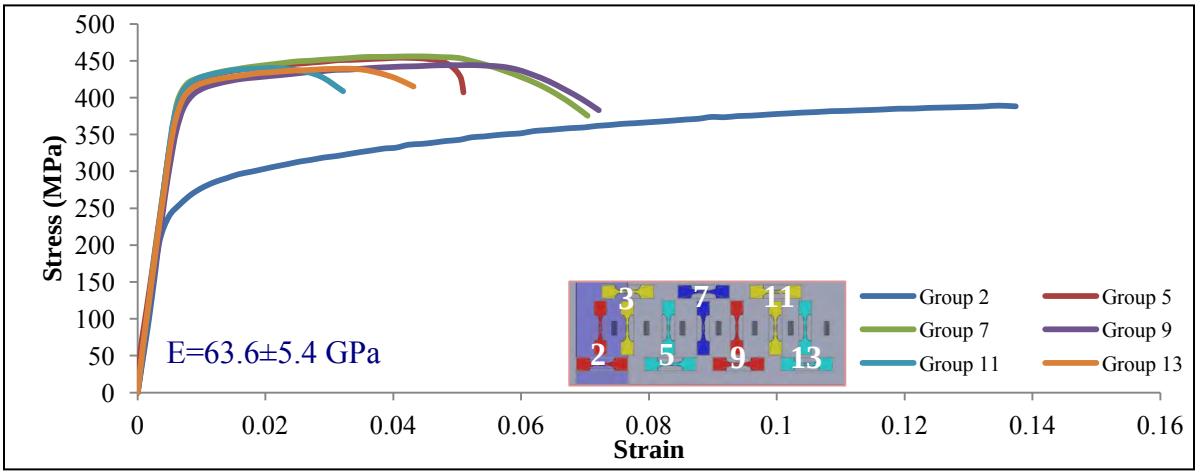

Figure 3. Tensile results in the Y-direction.

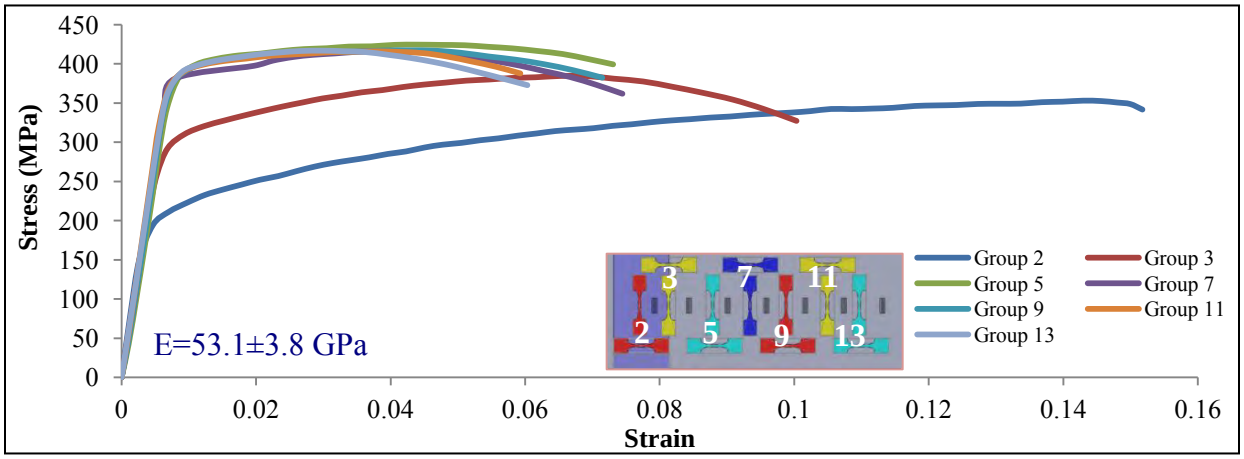

Figure 4. Tensile results in Z-direction.

Conversely, groups 5 and higher showed remarkable similarities in behavior in failure strain as well as ultimate tensile strength and elongation to failure in all directions. This would indicate that there are only spatial considerations for mechanical properties in the direct area of the weld.

A general trend was noticed that the modulus in the through thickness (Z) direction was the lowest in all the samples. This is most likely a result of the texturing in the grains that develops during cold working (*10*) of the plates prior to welding and the texturing that is created by the severe plastic deformation that is created through the welding process (*11*).

3.2 Microscopy: Grain Structures

From the tensile results, the entirety of the center weld was polished and etched, and is shown macroscopically in figure 5. From these images, the various microstructural zones are shown in figure 6, which is a result of different etching rates due to changes in grain sizes. In figure 6, sections A and B show the microstructures that develop in the weld nugget; however, A and B show different grain sizes. This is a result of the heat flux gradient that is generated during welding since previous studies have shown that as much as 86% of the heat flux is generated from the shoulder of the tool (*12*). For this reason, finer grains are observed in section A due to less grain growth occurring as a result of less heat. Section C is the TMAZ, D is the HAZ, and E is the unaffected material. The transition between structures is sometimes very distinct, as between A/B and A/C, but is harder to distinguish, as in the case of C/D.

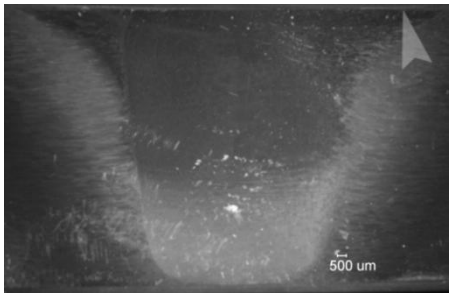

Figure 5. Post-etching image of weld.

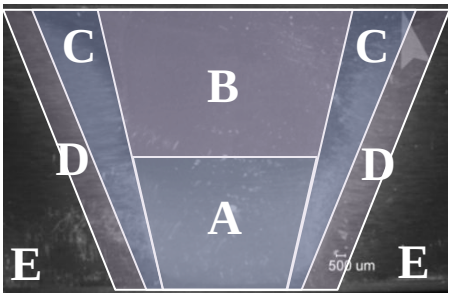

Figure 6. Post-etching image highlighting specific regions.

Examinations of the interfaces were done to show the distinct characteristics in the transition between zones and are shown in figures 7 and 8. Figure 7 shows a stark contrast between the very fine grains shown in section A of the weld nugget and the coarse grains of the TMAZ. This creates a very undesirable situation in which there is a large mismatch in mechanical properties. This mismatch during mechanical loading will cause an elevated local stress and likely lead to failure. The differences in A to B of the weld nugget are subtle, as shown in figure 8, but will still create an increased local stress at the interface with the TMAZ.

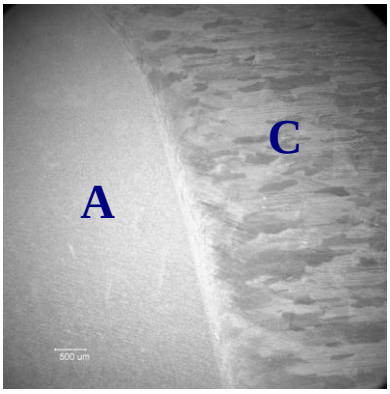

Figure 7. Transition between weld nugget and TMAZ.

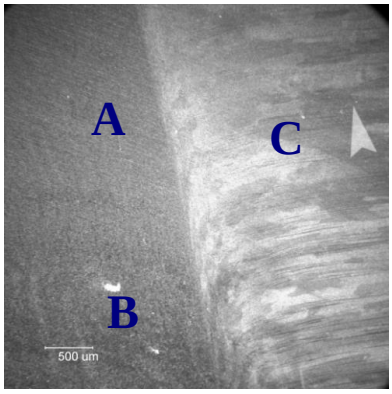

Figure 8. Transition inside of weld nugget and TMAZ.

Finally, the interface was once again examined to determine the relative difference in grain structures between the interfaces, as shown in figure 10. From figure 9, the fine equiaxed grains have an average grain size around 10–20 microns, while partially elongated grains on the major axis of the TMAZ, shown in figure 11, have a significantly larger grain size of over 100 microns. This once again shows a large and sudden change in the grain structure, which would lead to an elevated localized stress.

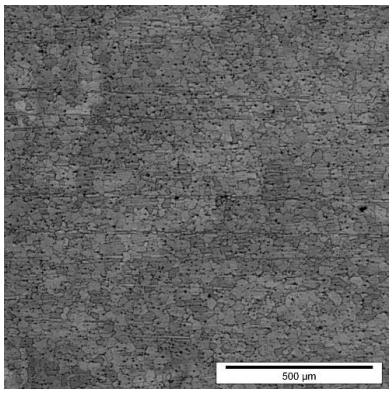

Figure 9. Fine equaixed grains observed in the weld nugget.

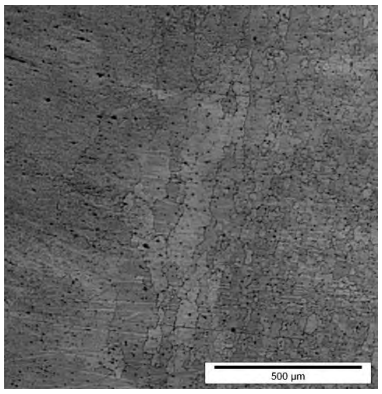

Figure 10. Transition between weld nugget and TMAZ.

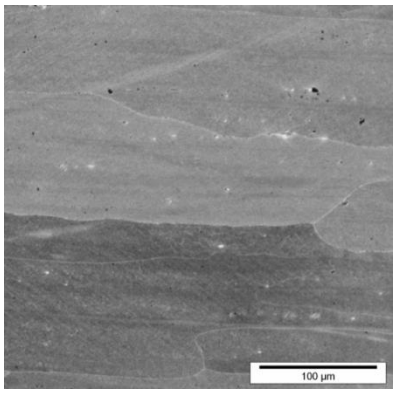

Figure 11. TMAZ zone showing elongated grains.

The existence of higher stresses caused by dissimilar mechanical properties can be seen in the results of the tensile test for the samples from region 2 and 3, shown in figures 2 through 4. From the current study, tensile specimens in the X-direction from region 2 would traverse the entire length of the weld, which would result in a very fine equiaxed grain structure through the gauge section, as that shown in figure 9. The Hall-Petch relationship indicates that yield stress would be higher than that of large grained materials shown in regions 5–13 (*14*). This, however, is not observed and is in fact calculated as a lower value. This would indicate that the yield strength, as characterized by Hall-Petch, must have been reached in order to cause plastic flow in the gauge section. The mismatch in material parameters causes elevated local stresses at the interface, which allows failure to occur.

3.3 Electron Backscatter Diffraction: Grain Analysis of Upper Weld Nugget

EBSD was performed on a sample taken from the *x-y* plane in upper part of the weld nugget. The as-imaged scanning electron microscopy (SEM) photo is shown in figure 12. Scratching of the sample was observed; however, it did not affect the ability to detect the grains, as shown in figure 13, which accurately mapped the grain boundaries. Figure 14 shows the results of the EBSD analysis. This shows that the grains are slightly elongated in the upper part of the nugget in the direction of the tool path. This is most likely a result of a dynamic recrystallization process taking place as the tool is passing through. This would result in texturing of grains in the Y-direction, which would result in directional hardening. These results are consistent with the findings of Medintz (*13*), the elongation to failure and ultimate tensile strength are higher for the X-direction, while modulus stays generally intact.

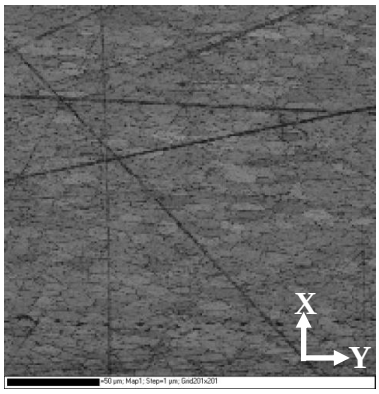

Figure 12. The as-imaged SEM.

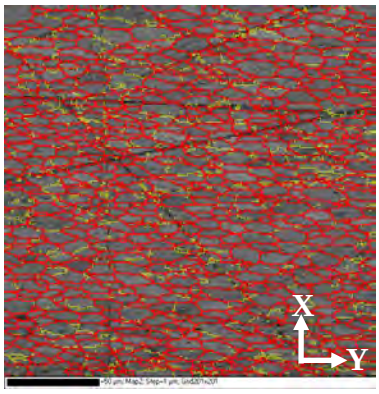

Figure 13. Identification of grain boundaries.

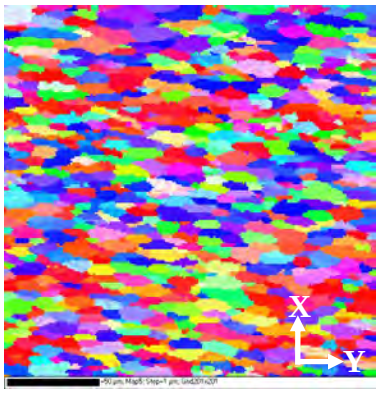

Figure 14. EBSD results.

The results of the pole analysis shown in figure 15 showed that the grains were generally well distributed in the crystallographic directions; however, there was slight preferential alignment toward the 101 and 111 directions. This may account for the anisotropic behavior of the tensile testing. The Z-direction shows a slight preferential orientation towards the 101 direction. This accounts for the lower modulus observed in the Z-direction as reported by Medintz (*13*). This is due to the fact that the single crystal of aluminum shows a highest modulus along the 111 direction (*14*). Having fewer grains aligned in this direction would lead to an overall lower relative modulus. This accounts for some of the issues related to the anisotropy found in testing.

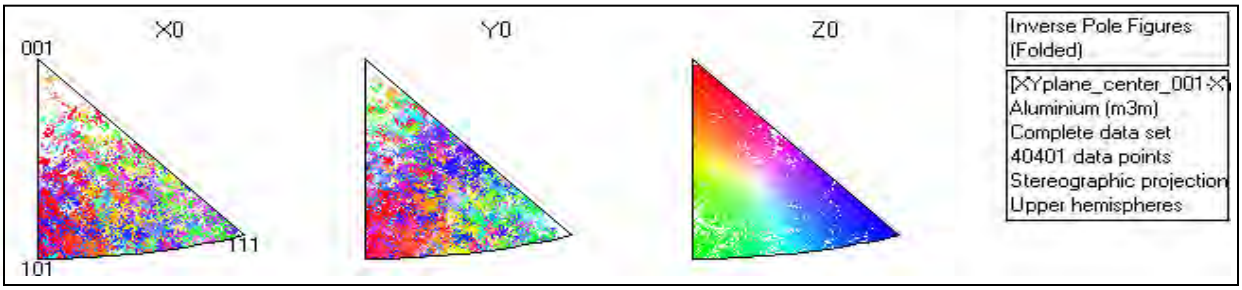

Figure 15. Results of grain analysis.

3.4 Observations on Increased Ductility

As seen from figures 2 through 4, the area in and around the weldment, shown in regions 2 and 3, exhibits the largest failure strain and highest ductility. When taking the strain fields from ARAMIS and plotting them during the elastic region, this phenomenon can be explained by the aforementioned work, in particular, the difference in microstructure. After plasticity occurs, geometric instabilities develop, which does not accurately characterize the strain distribution. These results are shown in figures 16 through 18. When comparing the results of the tensile test to the strain profiles along the tensile direction, it can be seen that this is a result of the microstructural distribution along the tensile axis.

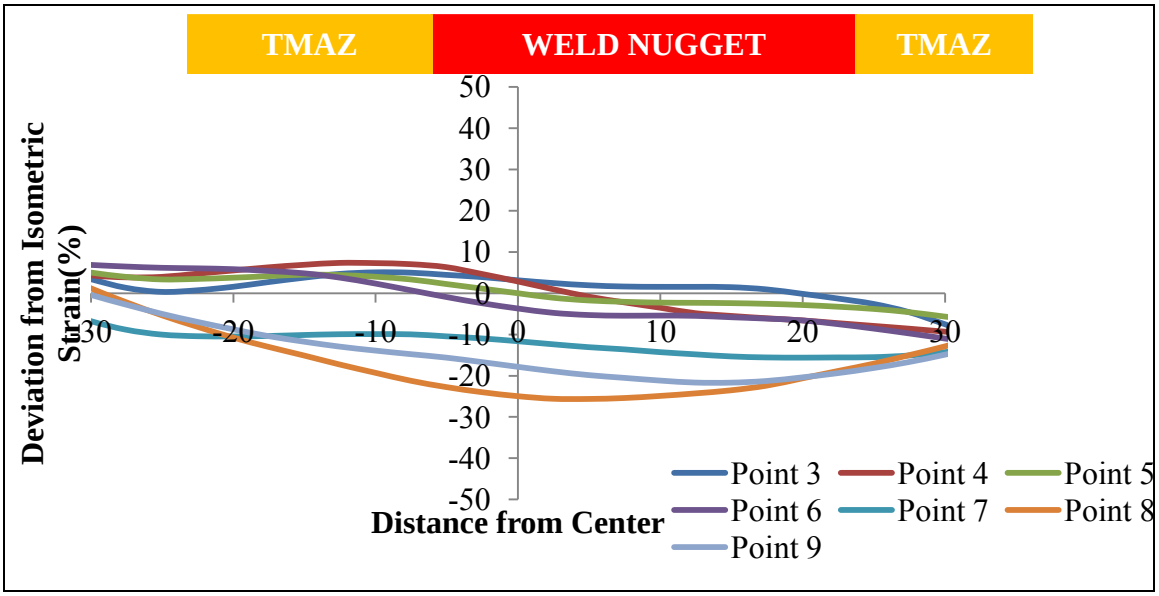

Figure 16. Strain distribution evolution in 2X from center weld.

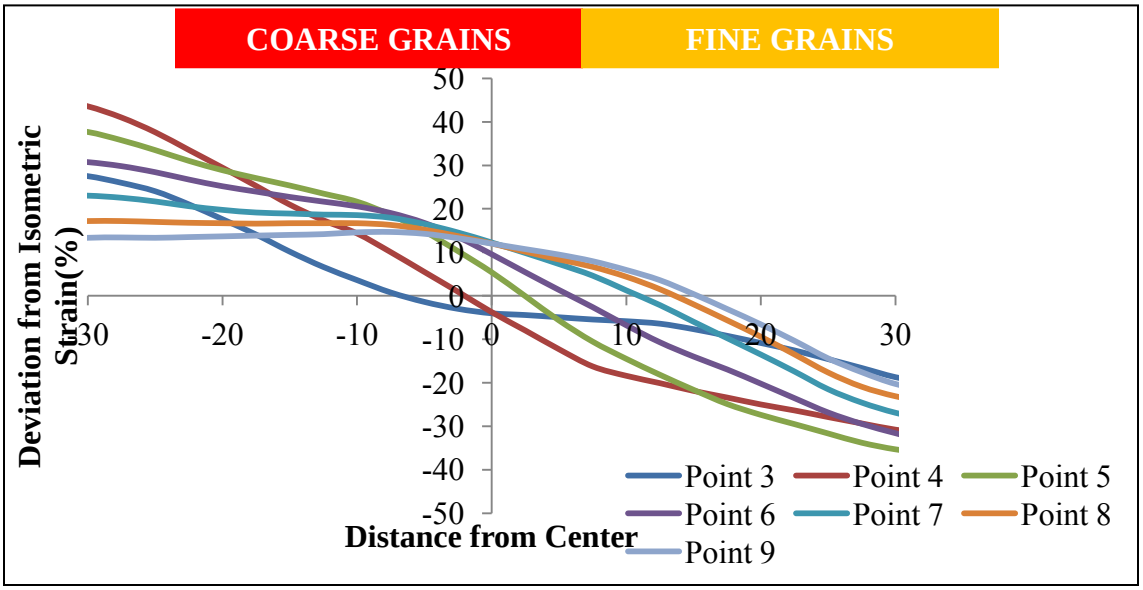

Figure 17. Strain distribution evolution in 2Z from center weld.

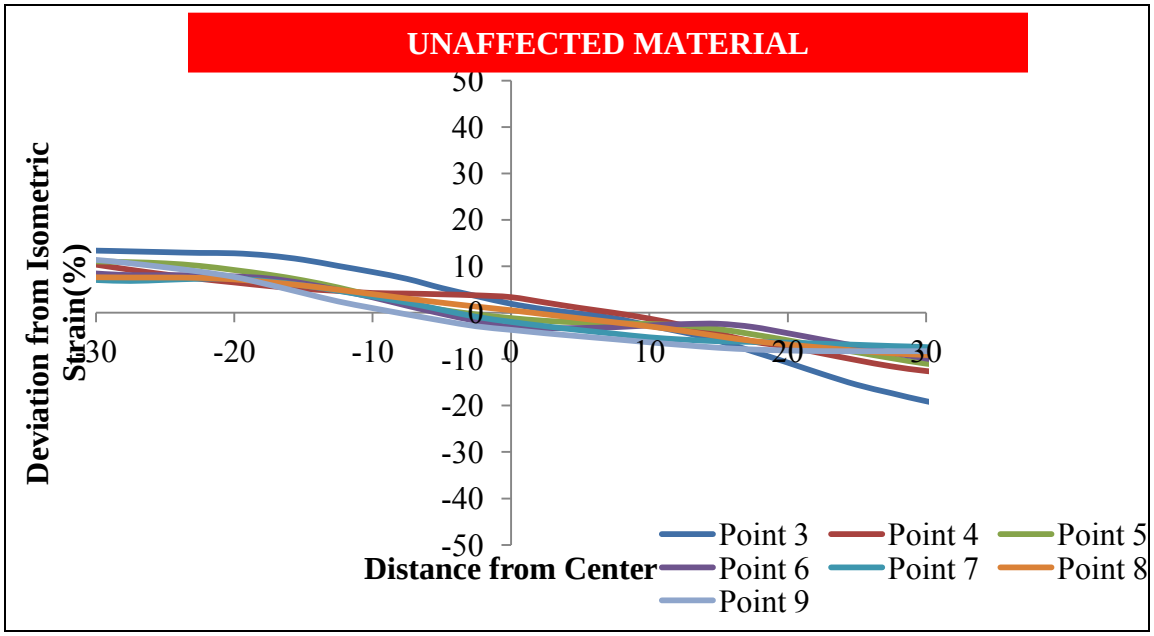

Figure 18. Strain distribution evolution in 11X.

The results from figure 16 indicate that as the material is strained, it does not strain isometrically, but rather is dependent on the microstructure in the given specimen. From figure 16, the center of the specimen strains at a rate 25% lower than the specimen average. This is related to the fine grains located in the center of the weld nugget.

The coarse grains of the TMAZ are straining at a higher gradient because of the grain size effect. These results demonstrate the development of local yielding in the more favorable zones. As indicated, the microstructurally related strain distribution evolution develops as the preferential grain structure begins to yield, in this case, the TMAZ. This result is in agreement with the Hall-Petch relationship (*14*).

Likewise, this same behavior is seen in the Z-direction of the weld and shows a distinct zone of both fine and coarse grains. This grain distribution effect on non-isometric strain is captured in figure 17, which shows the evolution of the strain distribution in the 2Z sample. As the strain distribution evolves, a preference toward straining is observed by the top nugget, which strains 12% higher than the average, whereas the bottom nugget strains as much as 15% below average. This again is an effect of the grain size. The finer grains are stronger and strain less than the coarse grains. This once again is in agreement with the Hall-Petch relationship.

Lastly, the strain distribution of the unaffected material far from the weld of section 11 is shown in figure 18. These results show that while there is slight preferential straining toward the top end of the sample, this pattern generally stays intact and there is no microstructural related strain evolution that develops during elastic loading. These results confirm the existence of a microstructural-related strain distribution evolution between zones in the weldment.

4. Summary and Conclusions

4.1 Summary

Tensile specimens were cut from an FSW butt joint of AA-2139 and tested. The mechanical properties show little spatial variation; however, in the weldment, there are significantly different mechanical properties. There is a higher failure strain and lower ultimate tensile strength in the weld zone. This may be attributed to the specific microstructures that form during the FSW process characterized by the TMAZ, HAZ, and weld nugget. Optical microscopy showed an abrupt change in the microstructure, which results in elevated local stresses due to the mismatch in mechanical properties. Additionally, a difference in local strain gradients was observed due to the microstructural differences, which allows for increased ductility. Analysis of the grain structure in these zones shows that the grains have a slight preferential alignment in the weld direction, which may account for the higher strains to failure. Anisotropic behavior can be explained by the preferential alignment of the grains towards the 101 and 111 directions in the X- and Y-directions while a preference toward the 101 is observed for the Z-direction.

4.2 Future Work

Since a model has been developed to accurately simulate the welding and relative microstructures, a novel technique for simulating the blast is needed. One way to do this would be to develop a homogenized response characterized by the spatial mechanical response of the weld. In order to do this, a better understanding of the mechanical properties derived in this experiment would be necessary. Further testing to understand the mechanical response in the weld zone will allow for successful implementation of the data into a homogenized center weld zone that will not require modeling of the TMAZ, HAZ, and weld nugget. When this is completed, a finite element model and simulation will be used to allow for a better design methodology to implement a FSW join on a vehicle.

5. References

1. Thomas, W. M.; Nicholas, E. D.; Needham, J. C.; Murch, M. G. Friction Stir Butt Welding. Patent Application Number 5,460,317 United States of America, 1995.

2. Mahoney, M. W.; Rhodes, C. G.; Flintoff, J. G.; Spurling, R. A.; Bingel, W. H. Properties of Friction-Stir-Welded 7075 T651 Aluminum. s.l.: *Metalurgical and Materials Transactions A* **July 1998**, *29A*.

3. Hirata, T.; Oguri, T.; Hagino, H.; Tanaka, T. Influence of Friction Stir Welding Parameters on Grain Size and Formability in 5083 Aluminum. 1-2, s.l.: *Material Science & Engineering A* **2007**, *456*, 334–349.

4. Buffaa, G.; Fratinia, L.; Shivpurib, R. CDRX Modelling in Friction Stir Welding of AA7075-T6 Aluminum Alloy: Analytical Approaches. 1-3, s.l.: *Journal of Materials Processing Technology*, *191*, 356–359.

5. Fratini, L.; Buffa, G. CDRX Modelling in Friction Stir welding of Aluminium Alloys. 10, s.l.: *International Journal of Machine Tools and Manufacture*, *45*, 1188–1194 .

6. Fratini, L.; Buffa, G.; Palmeria, D. *Computers & Structures.* 17–18, *87*, 1166–1174.

7. Grujicic, M.; Arakere, G.; Yalavarthy, H. V.; He, T.; Yen, C.-F.; Cheeseman, B. A. Modeling of AA5083 Material-Microstructure Evolution During Butt Friction-Stir Welding. s.l.: *Journal of Materials Engineering and Performance* **July 2010**, *19*, 672–684.

8. Grujicic, M.; Arakere, G.; Yen, C.-F.; Cheeseman, B. A. Computational Investigation of Hardness Evolution during Friction-Stir Welding of AA5083 and AA2139 Aluminum Alloys. s.l.: *Journal of Materials: Design and Applications* **January 2010**.

9. Grujicic, M.; Arakere, G.; Pandurangan, B.; Hariharan, A.; Yen, C-F.; Cheeseman, B. A.; Fountzoulas, C. Computational Analysis and Experimental Validation of the Ti-6Al-4V Friction Stir Welding Behavior. s.l.: *Journal of Engineering Manufacture January 2010*.

10. Yuana, H.; Wanga, Q. F.; Zhanga, J. W.; Liua, W. C.; Gaob, Y. K. Effect of Grain Shape on the Texture Evolution During Cold Rolling of Al–Mg Alloys. s.l.: *Journal of Alloys and Compounds* **2011**, *508*, 922–928.

11. Suhuddin, U.F.H.R.; Mironov, S.; Sato, Y. S.; Kokawa, H. Grain Structure and Texture Evolution During Friction Stir Welding of Thin 6016 Aluminum Alloy Sheets. s.l.: *Materials Science and Engineering A* **2010**, *527*, 1962–1969.

12. Schmidt, H.; Hattel, J.; Wert, J. An Analytical Model for the Heat Generation in Friction Stir Welding. s.l.: *Modelling and Simulation in Material Science and Engineering* **2004**, *12*, 143–157.

13. Medintz, J. Private Communication. US, ARL: s.n., July 2011.

14. Callister, William D.; Rethwisch, David G. *Materials Science and Engineering: An Introduction;* s.l.: John Wiley & Sons, 2009.